

# Crossing bonds in the random-cluster model

Wenan Guo <sup>1</sup> Youjin Deng <sup>2</sup> Henk W.J. Blöte <sup>3</sup>

<sup>1</sup>*Physics Department, Beijing Normal University, Beijing 100875, P. R. China*

<sup>2</sup>*Hefei National Laboratory for Physical Sciences at Microscale,  
Department of Modern Physics, University of Science  
and Technology of China, Hefei 230027, China and*

<sup>3</sup>*Lorentz Institute, Leiden University,  
P. O. Box 9506, 2300 RA Leiden, The Netherlands*

(Dated: March 27, 2009)

## Abstract

We derive the scaling dimension associated with crossing bonds in the random-cluster representation of the two-dimensional Potts model, by means of a mapping on the Coulomb gas. The scaling field associated with crossing bonds appears to be irrelevant, on the critical as well as on the tricritical branch. The latter result stands in a remarkable contrast with the existing result for the tricritical  $O(n)$  model that crossing bonds are relevant. In order to obtain independent confirmation of the Coulomb gas result for the crossing-bond exponent, we perform a finite-size-scaling analysis based on numerical transfer-matrix calculations.

PACS numbers: 05.50.+q, 64.60.Cn, 64.60.Fr, 75.10.Hk

## I. INTRODUCTION

In general one may expect that there exist large regions in the parameter space of the Hamiltonian of a critical system that belong to a single universality class. Or, stated in a different way, the critical exponents do, in general, not depend on the microscopic details of the Hamiltonian. The microscopic details will usually only contribute to the irrelevant fields as defined in the renormalization theory [1], and thereby influence the correction-to-scaling amplitudes. It is therefore surprising that it was found that the introduction of next-nearest-neighbor interactions in certain two-dimensional  $O(n)$  models, specified below, does affect the *leading* critical behavior.

In most exactly solved  $O(n)$  loop models, the loops do not cross or intersect, so that the loops are not entangled. The introduction of next-nearest-neighbor interactions, i.e., crossing bonds, in the square-lattice  $O(n)$  model leads, however, to a different situation. The crossing of two different loops segments produces a ‘defect’ that can be neutralized at a second crossing of the loop segments, or at an ordinary vertex where two of the loop segments emerging from the intersection point connect. Here the word ‘intersection’ refers to the projection of the loop segments on a planar lattice, the two loop segments should be considered as to remain separated from one another.

In the analysis of connected correlation functions between two crossings, one has to treat these loop crossings as topological defects, i.e., the annihilation of a defect at an ordinary vertex has to be disabled. Thus, we have a vertex with four outgoing loop segments at position 0, and the four segments come in at a vertex at position  $r$ . It is the ‘watermelon’ diagram with four lines.

After a mapping on the Coulomb gas, these two loop crossings are represented by known electric and magnetic charges [2, 3], so that the renormalization exponent associated with the fugacity of the crossings follows immediately. It is the same exponent as the one describing cubic crossover in the  $O(n)$  model,  $y = 2 - 2g + (1 - g)^2/(2g)$ , where  $g$  is related to  $n$  by  $n = -2\cos(\pi g)$ , with  $1 < g < 2$  for the critical branch, and with  $0 < g < 1$  for the low-temperature branch. It is irrelevant in the critical two-dimensional  $O(n)$  model with  $n < 2$ , but it becomes marginal at  $n = 2$ , and relevant in the low-temperature branch of the  $O(n)$  model [2]. It was found by Jacobsen et al. [4] that crossing bonds do indeed induce crossover to a new universality class [5] in the low-temperature branch. Another recent

result establishes a relation between the partition sum of the low-temperature branch of the  $O(n)$  model and that of a tricritical  $O(n)$  model [6]. The exponent associated with crossing bonds remains unchanged under this mapping. Therefore, crossing bonds are relevant in the tricritical  $O(n)$  model. However, the case  $n = 1$ , i.e. the tricritical Ising model, is not believed to be unstable with respect to crossing bonds, and is therefore interpreted as a special case, apparently because the truncation of the spin dimensionality to  $n = 1$  in effect eliminates the amplitudes associated with the effects of scaling fields acting on the other spin components.

These findings for the low-temperature and the tricritical  $O(n)$  model raise the question what are the consequences of crossing bonds in the two-dimensional Potts model [7, 8] and the equivalent random-cluster model [9], and also in the related tricritical models. The Potts model is defined in terms of lattice variables  $\sigma_i$  that can assume the discrete values  $1, 2, \dots, q$ , and the index  $i$  refers to the lattice site. The reduced Hamiltonian of the model is

$$\mathcal{H}/k_{\text{B}}T = -K \sum_{\langle ij \rangle} \delta_{\sigma_i, \sigma_j}, \quad (1)$$

where  $K$  is the Potts coupling, inversely proportional to the temperature. The summation indicated by  $\langle ij \rangle$  is over all interacting nearest-neighbor pairs of Potts variables. A generalization to continuous  $q$  is obtained by mapping this model (1) onto the Kasteleyn-Fortuin random-cluster model [9], whose partition sum is

$$Z(q, K) = \sum_{\{b\}} u^{n_b} q^{n_c}, \quad (2)$$

where the sum is over all graphs  $\{b\}$  formed by independent bond variables (absent or present), the bond weight is given by  $u = 1 - e^{-K}$ ,  $n_b$  is the number of present bonds, and  $n_c$  is the number of clusters formed by these bonds. The number  $q$  of Potts states now appears as a continuous variable, so that the random-cluster model can be seen as a generalization of the Potts model. In the limit  $q \rightarrow 1$  it reduces to the bond-percolation model. The presence of crossing bonds in a percolation model [10] has been investigated, but that work did not yield evidence for a possible modification of the finite-size-scaling behavior.

This question about the effects of crossing bonds in this model will be answered below. In Sec. II we derive the scaling dimension associated with crossing bonds analytically, with the

help of a renormalization mapping of the Potts model on the Coulomb gas. The validity of this analytic result is checked numerically in Sec. III, by means of a transfer-matrix analysis combined with finite-size scaling. A short discussion in Sec. IV concludes this paper.

## II. COULOMB GAS

The mapping of the random-cluster model on the Coulomb gas involves, as a first step, the representation of the random clusters by means of loops on the surrounding lattice. For a random-cluster model without crossing bonds, one obtains a system of non-intersecting loops [11]. Let us now consider the ‘defect’ introduced by the crossing or intersection of two random-cluster bonds. The four random-cluster bond segments going out from the intersection point are represented by eight outgoing loop segments. This is an important difference with the  $O(n)$  loop model, where one has four outgoing loop segments. While these crossing bonds introduce an entangled random-cluster configuration, the entanglement can be eliminated at ordinary vertices where random-cluster bonds meet. However, we are interested in the connected correlation function  $g(r)$  associated with two of these crossing-bond vertices separated by a distance  $r$ . Thus, we have to treat the defects as topological defects, and disable the annihilation of entanglement at ordinary vertices. The two special vertices are connected by four different random clusters. In the language of the surrounding loop model, we have to analyze the watermelon diagram with eight legs, as illustrated in Fig. 1.

In the Coulomb gas, both of these vertices are represented by a charge consisting of an electric and a magnetic component [2]. At position 0 and  $r$ , these charges are denoted  $(e_0, m_0)$  and  $(e_r, m_r)$  respectively. Here,  $m_0 = -m_r = 4$  is half the number of loop segments of the watermelon diagram, and  $e_0 = e_r = 1 - g$  is determined by the Coulomb gas coupling constant  $g$  which is known as a function of the number of Potts states of the critical random-cluster model:

$$g = 1 - \frac{1}{2\pi} \arccos \left( \frac{q}{2} - 1 \right) . \quad (3)$$

The decay of the correlation function  $g(r)$  as a function of  $r$  is as  $g(r) \propto r^{-2X_x}$ , governed by the scaling dimension  $X_x$ . The scaling dimensions associated with a general pair of charges

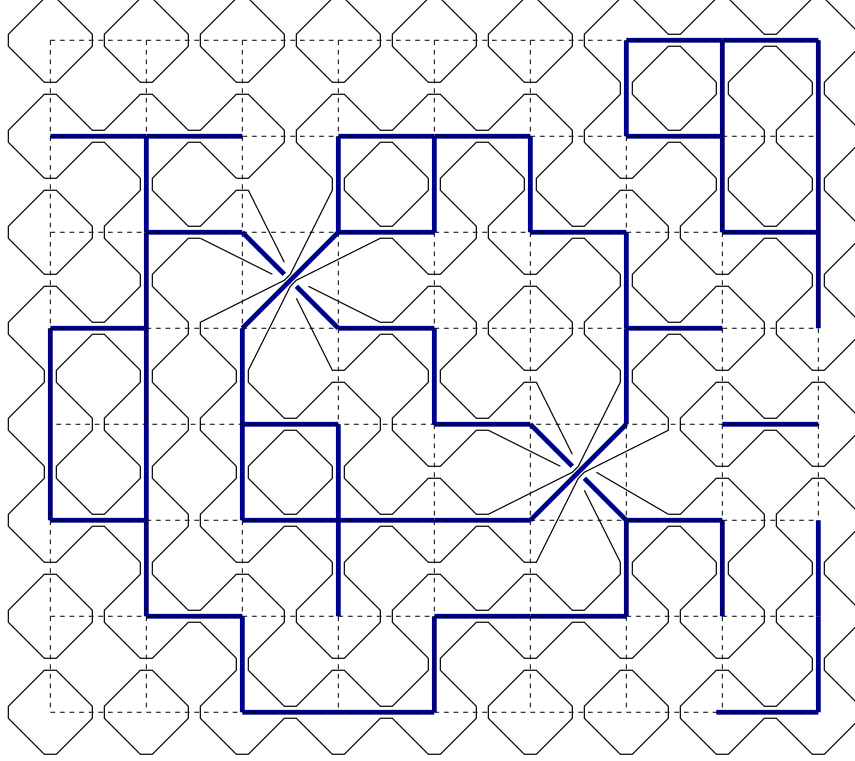


FIG. 1: Random-cluster configuration with two crossing-bond vertices, and the corresponding loop configuration on the surrounding lattice. The two vertices are connected by four random clusters, each of which is surrounded by two loop segments. The two vertices are thus connected by eight loop segments.

is given by

$$X(e, m) = -\frac{e_0 e_r}{2g} - \frac{m_0 m_r g}{2} \quad (4)$$

which implies, in the present case,

$$X_x = 1 - \frac{1}{2g} + \frac{15g}{2}. \quad (5)$$

### III. TRANSFER-MATRIX ANALYSIS

Transfer-matrix calculations usually apply to a system wrapped on a cylinder with a finite circumference  $L$ , while the limit is taken of an infinite length. In transfer matrix calculations on random-cluster models, the concept of ‘connectivity’ is an essential ingredient. For a square-lattice model with only nearest-neighbor couplings, wrapped on a cylinder with an open end, there are  $L$  sites located at this end. Sites that belong to the same cluster are

said to be connected. Each of the  $L$  end sites can thus be connected to zero or more other end sites; the precise way in which the end sites are connected is called ‘connectivity’. These connectivities can be coded by means of subsequent integers, which then serve as a transfer-matrix index. We denote the partition sum of a model with  $L \times M$  sites on a cylinder as  $Z^{(M)}$ . Then,  $Z^{(M)}$  can be divided into a number of restricted sums according to the index  $\alpha$  of the connectivity of the  $M$ th row, i.e.,  $Z^{(M)} = \sum_{\alpha} Z_{\alpha}^{(M)}$ . Then, the restricted sums for a model with  $M + 1$  layers of  $L$  sites can be written as a linear combination of the restricted sums for a system with  $M$  layers [12]:

$$Z_{\alpha}^{(M+1)} = \sum_{\beta} T_{\alpha\beta} Z_{\beta}^{(M)} \quad (6)$$

where the coefficients  $T_{\alpha\beta}$  define the transfer matrix  $\mathbf{T}$ .

The number of connectivities for a finite size  $L$ , as well as the way they are coded, still depends on the type of random-cluster model. In the absence of a magnetic field, and for nearest-neighbor bonds only, the connectivities are ‘well nested’. This means that, if the end sites numbered  $i$  and  $j$  are connected, and  $k$  and  $l$  are connected, while the pair  $i, j$  is not connected to  $k, l$ , that the case  $i < k < j < l$  is excluded. The random-cluster bonds are not entangled. More details, including a full description of the coding algorithm, appear in Ref. 13.

### A. Entangled random clusters

The problem defined in Sec. I does, however require the introduction of entangled random-cluster configurations. For the general problem of a random-cluster model with crossing bonds, one has to provide a different coding algorithm which allows only the analysis of a very limited range of finite sizes [10], because of the rapid increase with  $L$  of the required number of connectivities. A better approach is the use of the ‘magnetic’ connectivities, also defined in Ref. 13, which enable the introduction of a nonzero magnetic field. While we are here not interested in the introduction of a field, we do use the property of these magnetic connectivities that they allow for one magnetic cluster that need not be well nested in combination with other clusters. The occurrence of one such a cluster is sufficient for our present purposes. The number of these magnetic connectivities increases less rapidly with  $L$  than that of the entangled connectivities used in Ref. 10 for a crossing-bond model.

In our transfer-matrix analysis, we have to perform the calculation of the exponent associated with the connected correlation function between two vertices with four outgoing random-cluster bonds. Thus there exist four random clusters, which are not mutually connected (except at the two vertices), and each of these clusters connects to precisely one outgoing bond of each of the two vertices. The calculation of this exponent can be done by means of transfer matrices, with the help of Cardy's conformal mapping [14] between the infinite plane and a cylinder with circumference  $L$ . The mapping of a conformally invariant model between these two geometries shows that the scaling dimension  $X_x$  describing the algebraic decay of the correlation function  $g(r) \propto r^{-2X_x}$  in the infinite plane is related to the length scale  $\xi_x(L)$  describing the exponential decay of the analogous correlation function with distance in the cylindrical geometry [14] as

$$X_x \simeq \frac{L}{2\pi\xi_x(L)}. \quad (7)$$

For a system at criticality, this relation may be expected to hold only in the limit of  $L \rightarrow \infty$ , because the irrelevant fields that are usually present cause deviations from the conformal symmetry. But, in many cases, the calculation of  $\xi$  for a limited number of system sizes still allows a reasonably accurate estimate of the scaling dimension  $X$ . The correlation length  $\xi_x(L)$  is related to an eigenvalue  $\Lambda_x$  of the transfer matrix as

$$\xi_x^{-1}(L) = \zeta \ln \frac{\Lambda_0(L)}{\Lambda_x(L)} \quad (8)$$

where where the geometrical factor  $\zeta$  (the ratio between the unit of  $L$  and the thickness of a layer added by  $\mathbf{T}$ ),  $\Lambda_0(L)$  is the largest eigenvalue of  $\mathbf{T}$ , and  $\Lambda_x(L)$  the eigenvalue associated with the connected correlation function between the two vertices. One of the remaining tasks is thus to identify the latter eigenvalue in the spectrum of  $\mathbf{T}$ .

## B. Block structure of the transfer matrix

To determine the eigenvalue  $\Lambda_x(L)$ , we divide the connectivities in two groups: the first group contains the well-nested ones labeled by a subscript w, and the second group the entangled ones, labeled by a subscript e. The transfer matrix can then, in obvious notation, be divided in four blocks as

$$\mathbf{T} = \begin{bmatrix} \mathbf{T}_{ww} & \mathbf{T}_{we} \\ \mathbf{0}_{ew} & \mathbf{T}_{ee} \end{bmatrix}, \quad (9)$$

where the lower left block contains only zeroes, because the Hamiltonian does not contain crossing bonds, and the transfer matrix is thus unable to form entangled states out of well-nested ones. As a consequence, the *transpose* transfer matrix  $\mathbf{T}^t$  cannot form well-nested states out of entangled ones. The eigenvalue problem of  $\mathbf{T}$  in effect decomposes in the two separate eigenvalue problems of  $\mathbf{T}_{\text{ww}}$  and  $\mathbf{T}_{\text{ee}}$ . Our algorithm to find the eigenvalues [13] is based on the analysis of a sequence of vectors obtained by the repeated multiplication of an initial vector by  $\mathbf{T}^t$ . Thus, if we use an initial vector that contains only entangled states, we easily obtain the largest eigenvalue of the diagonal block  $\mathbf{T}_{\text{ee}}$ . Naturally, the largest eigenvalue of  $\mathbf{T}_{\text{ee}}$  will be associated with the ‘least entangled states’ in which only two clusters are entangled, as for instance the four-site connectivity in which site 1 is connected to 3, and 2 to 4. That is precisely the set of connectivities describing the correlation between two of the aforementioned vertices, which, in the geometry of an infinitely long cylinder, are thought to be located at  $\pm\infty$ .

### C. Finite-size analysis

The eigenvalues  $\Lambda_0(L)$  and  $\Lambda_x(L)$  were calculated numerically as described above, for finite sizes up to  $L = 15$ , for which the number of connectivities is 390 248 055. This was done for two different transfer matrices. First, we chose the transfer direction parallel to a set of lattice edges, and second, we chose it in the direction of a set of diagonals of the elementary faces of the square lattice. The latter method can handle larger system sizes when expressed in lattice edges, although the number of finite sizes is the same. Since the finite-size parameter  $L$  denotes the number of sites added by a multiplication by  $\mathbf{T}^t$ , the circumference of the cylinder is  $L$  lattice edges for the ‘parallel’ transfer matrix, and  $L\sqrt{2}$  lattice edges for the ‘diagonal’ transfer matrix. The geometric factors are  $\zeta = 1$  and  $\zeta = 1/2$  respectively, because we express  $\xi_x(L)$  in the same units as  $L$ .

A convenient quantity in the finite-size analysis is the ‘scaled gap’ which depends here (except on the type of the transfer matrix) only on  $L$ , because the Potts coupling is set at its critical value. This quantity is defined as

$$X_x(L) = L/[2\pi\xi_x(L)]. \quad (10)$$



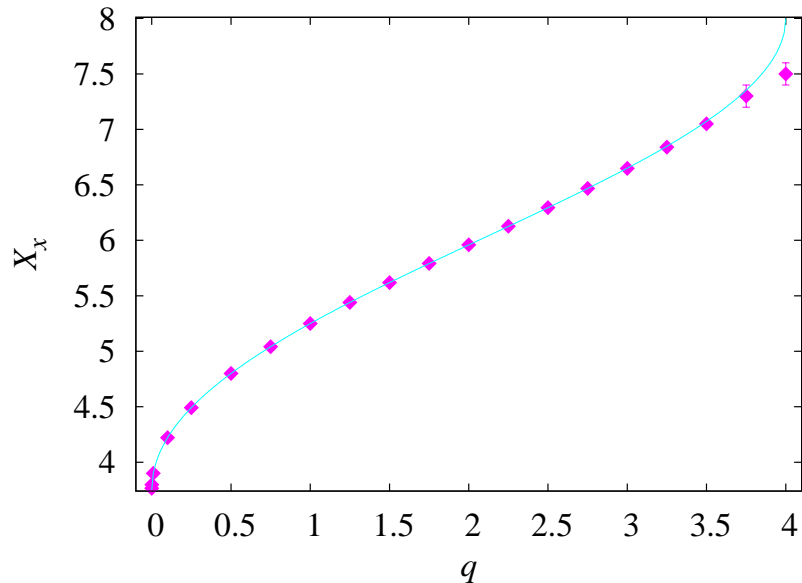


FIG. 2: Results for the scaling dimension  $X_x$  associated with crossing bonds in the random-cluster model, as a function of the number  $q$  of Potts states. The symbols show the averages of the numerical results obtained from the two transfer matrices. The curve shows the Coulomb gas result.

In the vicinity of a renormalization fixed point, finite-size scaling leads to the equation

$$X_x(L) = X_x + a_u L^{y_u} + \dots \quad (11)$$

where  $y_u$  is an irrelevant exponent and  $a_u$  the associated finite-size amplitude, and the dots stand for further finite-size corrections. The first step of the estimation of the scaling dimension  $X_x$  is done by means of power-law fits according to this equation. The resulting estimates are expected to depend, again, on  $L$  as a power law. Thus, better estimates can be obtained by means of an iterated fitting procedure. Up to four iteration steps were made. We tried several variations of the fitting procedure, concerning the use of a-priori knowledge of the exponents of the finite-size dependences. We expect corrections described by the integer exponent  $-2$ , as well as by the irrelevant Potts exponent [2]. Further details appear in Refs. 13 and 15. The numerical uncertainties in  $X_x$  were roughly estimated from the variation of its fitted value with increasing system size. The best estimates, and the estimated error margins, are shown in Table I and Fig. 2, together with the theoretical values derived in Sec. II.

TABLE I: Results of transfer-matrix calculations for the crossing-bond dimension. The numerical results for  $X_x$  are indicated by the superscript ‘num’. They were determined using two different transfer-matrix methods: with the transfer direction parallel to a set of edges of the square lattice, as indicated by ‘(e)’, and with transfer direction parallel to a set of diagonals of the elementary faces, as indicated by ‘(d)’. The estimated error in the last decimal place is shown between parentheses. For comparison we also show the Coulomb gas prediction in the last column.

$q$	$X_x^{\text{num}}(\text{e})$ error	$X_x^{\text{num}}(\text{d})$ error	$X_x^{\text{theory}}$
0.0001	3.76511 (1)	3.765110 (2)	3.765110
0.001	3.79772 (1)	3.797715 (2)	3.797714
0.01	3.90028 (1)	3.900277 (2)	3.900278
0.10	4.22087 (1)	4.220862 (5)	4.220863
0.25	4.49180 (2)	4.49180 (1)	4.491800
0.50	4.7997 (1)	4.79970 (5)	4.799728
0.75	5.0411 (1)	5.0410 (1)	5.040971
1.00	5.2500 (1)	5.2500 (1)	5.250000
1.25	5.4404 (1)	5.4404 (1)	5.440283
1.50	5.6190 (2)	5.6192 (2)	5.618945
1.75	5.790 (1)	5.7912 (5)	5.790520
2.00	5.957 (1)	5.959 (1)	5.958333
2.25	6.123 (2)	6.127 (2)	6.125203
2.50	6.290 (5)	6.295 (2)	6.293876
2.75	6.46 (1)	6.468 (2)	6.467453
3.00	6.63 (2)	6.648 (5)	6.650000
3.25	6.80 (5)	6.84 (1)	6.847755
3.50	7.1 (1)	7.05 (1)	7.072311
3.75	7.3 (2)	7.3 (1)	7.353038
4.00	7.4 (5)	7.5 (1)	8.000000

## IV. DISCUSSION

The introduction of next-nearest-neighbor couplings in Potts models increases the size of the transfer matrix, and thus leads to new eigenvalues of which we have associated one with the scaling dimension  $X_x$ . Our analysis was only focused on the determination of  $X_x$ . Of course, the appearance of effects described by this scaling dimension is only one of the consequences. The new couplings do also increase the range of the interactions, and this influences the irrelevant field and its associated corrections to scaling [16]. This effect is well known and outside the scope of the present paper.

Most of the numerical data in Table I agree well with the Coulomb gas prediction. But it is clear that the agreement deteriorates near  $q = 4$ , where the error estimates become quite large, but not large enough to explain the difference with the Coulomb gas result. This problem is explained in terms of the behavior of the second thermal exponent of the Potts model, which is strongly irrelevant for small  $q$ , but increases with  $q$  and becomes marginal at  $q = 4$ . This explains why the fast convergence at small  $q$  deteriorates for larger  $q$ , in particular at  $q = 4$  where a logarithmic correction factor leads to misleading finite-size fits, which assume a power-law behavior instead. We thus conclude that our numerical analysis is in agreement with the theoretical predictions.

The consistency between the theory and the numerical results for the scaling dimension associated with crossing bonds is quite reassuring. However, a strange aspect of the present result is that it seems inconsistent with the equivalence between the  $O(1)$  model and the  $q = 2$  Potts or random-cluster model. Both of these are Ising models, and one may thus expect to find the same scaling dimension for crossing bonds. For the critical  $O(1)$  model, one finds  $X_x = 21/8$  [2], whereas Eq. (5) yields  $X_x = 143/24$ . To answer this paradox one may note that, for the Ising case, the scaling behavior of the thermodynamic observables is determined by a very limited set of scaling fields associated with primary operators in the conformal field theory [17]. The critical amplitudes associated with other scaling fields vanish in thermodynamic quantities but may appear in e.g. the fractal dimensions of spin clusters or percolation clusters defined on the ensemble of configurations generated by Eqs. (1) and (2). The geometric correlations associated with crossing random-cluster bonds should naturally be different from those associated with crossing bonds in the  $O(1)$  model because the two corresponding Coulomb gas descriptions are based on two different graph expansions of the

Ising model.

In the notation based on the Kac formula [18] for the dimensions of rotationally invariant observables, namely

$$X_{p,q} = \frac{[p(m+1) - qm]^2 - 1}{2m(m+1)}. \quad (12)$$

where  $m = g/(1-g)$  for the critical Potts model, the Coulomb gas result Eq. (5) can be written

$$X_x = X_{0,4}. \quad (13)$$

This is outside the restricted set of operators [17] with  $1 \leq p < m$ ,  $1 \leq q < m+1$  which describe the thermodynamics of unitary models. Thus, for critical Potts models with integer  $q$ , effects described by the dimension  $X_x$  should be absent in the thermodynamic behavior, but may still appear in fractal and geometric properties of critical spin configurations.

Finally, we note that the Coulomb gas result Eq. (5) for the dimension  $X_x$  also applies to the tricritical branch of the random-cluster model, with  $g = 1 + \arccos(q/2 - 1)/(2\pi)$  instead of Eq. (3), which implies that the crossing bond dimension is even larger, i.e., more irrelevant, than that on the critical branch. We recall that, in contrast, the crossing-bond exponent is *relevant* in the tricritical  $O(n)$  model.

## Acknowledgments

We are indebted to Prof. B. Nienhuis for valuable discussions. H.B. gratefully acknowledges the hospitality of the Physics Department of the Beijing Normal University and the Modern Physics Department of University of Science and Technology of China. The research is supported by the Science Foundation of The Chinese Academy of Sciences, by the NSFC under Grant #10675021, by the Program for New Century Excellent Talents in University (NCET), and by the Lorentz Fund.

- 
- [1] K. G. Wilson, Phys. Rev. B **4**, 3174 (1971); K. G. Wilson, Phys. Rev. B **4**, 3184 (1971).
  - [2] B. Nienhuis, *Phase Transitions and Critical Phenomena*, edited by C. Domb and J.L. Lebowitz. (Academic, London, 1987), Vol. 11, p 1.
  - [3] H. Saleur and B. Duplantier, Phys. Rev. Lett. **58**, 2325 (1987).

- [4] J. L. Jacobsen, N. Read, and H. Saleur, Phys. Rev. Lett. **90**, 090601 (2003).
- [5] M. J. Martins, B. Nienhuis and R. Rietman, Phys. Rev. Lett. **81**, 504 (1998); M. J. Martins and B. Nienhuis, J. Phys. A **31**, L723 (1998).
- [6] B. Nienhuis, W.-A. Guo and H. W. J. Blöte, Phys. Rev. E **78**, 061104 (2008).
- [7] R. B. Potts, Proc. Cambridge. Philos. Soc. **48**, 106 (1952).
- [8] F. Y. Wu, Rev. Mod. Phys. **54**, 235 (1982).
- [9] P. W. Kasteleyn and C. M. Fortuin, J. Phys. Soc. Jpn. **46** (Suppl.), 11 (1969); C. M. Fortuin and P. W. Kasteleyn, Physica **57**, 536 (1972).
- [10] X. M. Feng, Y. Deng and H. W. J. Blöte, Phys. Rev. E **78**, 031136 (2008).
- [11] R. J. Baxter, S. B. Kelland and F. Y. Wu, J. Phys. A **9**, 397 (1976).
- [12] T.D. Schultz, D.C. Mattis and E.H. Lieb, Rev. Mod. Phys. **36**, 856 (1964).
- [13] H. W. J. Blöte and M. P. Nightingale, Physica A **112**, 405 (1982).
- [14] J. L. Cardy, J. Phys. A **17**, L385 (1984).
- [15] For reviews, see e.g. M. P. Nightingale in *Finite-Size Scaling and Numerical Simulation of Statistical Systems*, ed. V. Privman (World Scientific, Singapore 1990), and M. N. Barber, see Ref. [2] (Academic, London 1989), Vol. 8, p. 146.
- [16] F. J. Wegner, Phys. Rev. B **5**, 4529 (1972).
- [17] J. L. Cardy, see Ref. [2] (Academic Press, London, 1987), Vol. 11, p. 55.
- [18] D. Friedan, Z. Qiu and S. Shenker, Phys. Rev. Lett. **52**, 1575 (1984).